DOI: 10.18721/JPM
UDC 621.391:681.142

A TRIANGULATION SENSOR FOR MEASURING THE DISPLACEMENTS AND HIGH-PRECISION MONITORING OF THE PRODUCTION PERFORMANCE

V.A. Stepanov, E.N. Moos, M.V. Shadrin,
V.N. Savin, A.V. Umnyashkin, N.V. Umnyashkin

Ryazan State University named for S. Yesenin, Ryazan, Russian Federation

Using the method of laser triangulation as the base, a mobile high-precision sensor has been created for measuring displacements and monitoring of the geometric parameters of workpieces in production. Both the process of signal processing and the operation of the triangulation sensor were accelerated many times owing to the architecture of processes, which was based on a reduced set of commands using simple and effective instructions of the stm32f407vet6 microcontroller. The measurement procedure was carried out by searching for a laser spot, calculating the center of the spot using the center of mass method, converting the centroid into the metric and applying calibration tables. Sensor scan speed amounted to $(3 - 5)\cdot 10^3$ s^{-1}.

Keywords: triangulation sensor, microprocessor, laser diode, spot center, interface, control module

Citation: Stepanov V.A., Moos E.N., Shadrin M.V., Savin V.N., Umnyashkin A.V., Umnyashkin N.V., A triangulation sensor for measuring the displacements and high-precision monitoring of the production performance, St. Petersburg Polytechnical State University Journal. Physics and Mathematics. 13 (1) (2020) 47–58. DOI: 10.18721/JPM.13105

ТРИАНГУЛЯЦИОННЫЙ ДАТЧИК ДЛЯ ИЗМЕРЕНИЯ ПЕРЕМЕЩЕНИЙ И ВЫСОКОТОЧНОГО КОНТРОЛЯ ПАРАМЕТРОВ ИЗДЕЛИЯ НА ПРОИЗВОДСТВЕ

В.А. Степанов, Е.Н. Моос, М.В. Шадрин,
В.Н. Савин, А.В. Умняшкин, Н.В. Умняшкин

Рязанский государственный университет имени С.А. Есенина,

г. Рязань, Российская Федерация

На основе метода лазерной триангуляции создан мобильный высокоточный датчик для измерения перемещений и контроля геометрических параметров изделий на производстве. Архитектура процессов, построенная на сокращенном наборе команд, использующих простые и эффективные инструкции микроконтроллера stm32f407vet6, обеспечивает многократное ускорение не только процесса обработки сигнала, но и работы триангуляционного датчика. Процедура измерения осуществляется путем поиска лазерного пятна, расчета расположения центра пятна методом центра масс, перевода центроиды в метрику и применения калибровочных таблиц. Достигнутая скорость сканирования датчика составляет $(3 - 5)\cdot 10^3$ измерений в секунду.

Ключевые слова: триангуляционный датчик, микропроцессор, лазерный диод, центр пятна, интерфейс, модуль управления

Ссылка при цитировании: Степанов В.А., Моос Е.Н., Шадрин М.В., Савин В.Н., Умняшкин А.В., Умняшкин А.В., Умняшкин Н.В. Триангуляционный датчик для измерения перемещений и высокоточного контроля параметров изделия на производстве // Научно-технические ведомости СПбГПУ. Физико-математические науки. 2020. Т. 13. № 1. С. 54–65. DOI: 10.18721/JPM.13105

Introduction

The significance of this study stems from the need for high-precision monitoring of the movements of working bodies in machining centers in production and development of workpieces in such industries as engineering, aerospace industry, military production, as well as in other branches where precise control of geometric parameters or positions of the objects is required.

The triangulation method for measuring the displacements, geometric dimensions and roughness of workpieces with complex surfaces [1 – 6] was used to develop a sensor for measuring displacements and monitoring the geometric parameters of workpieces in dynamics, for example, on a conveyor, without slowing down production. The sensor must provide high accuracy for operation (control) in various industries and a high scanning speed; be compact and have a degree of protection appropriate to the needs of enterprises. The software can process signals from the measuring channel of the sensor transferring the main aspect in the development of applications from hardware to software.

The principle of triangulation distance measurement

The triangulation method of control is based on calculating the required distance in terms of the ratios in the triangle using known system parameters. This allows to measure both the relative change in the distance from the sensor to the controlled object and its absolute value.

The triangulation scheme (Fig. 1) can conditionally be divided into three parts: a radiating (or lighting) channel, a controlled surface, and a receiving channel.

The first part of the meter is a channel consisting of a radiation source and an objective lens, where a probe beam is formed on a controlled surface. A laser diode with a Gaussian distribution is typically used as such a source. The objective lens consists of one or more optical lenses. Its relative position and the position of the laser diode determine the setting of the emitting channel. To set up the laser module (for getting the maximum intensity value), it is necessary to set the constriction to the center of the measuring range and to center the probe beam. The result of good adjustment is a centered beam, whose width and intensity vary symmetrically relative to the center of the measurement range.

The second integral part of the triangulation meter is the controlled surface. Any surface reflects or scatters incident radiation. Scattering of radiation by the surface of a controlled object is used in triangulation as the basis for obtaining information about the distance to this surface.

The triangulation sensor is intended for measuring the distance from the selected point on the probe beam axis to the physical point on the surface with high accuracy. Any controlled surface is characterized by roughness, corresponding to the degree to which the surface is smooth or uneven. The required measurement accuracy is usually inversely proportional to the roughness of the surface monitored. In particular, the surface roughness of microelectronic crystals and

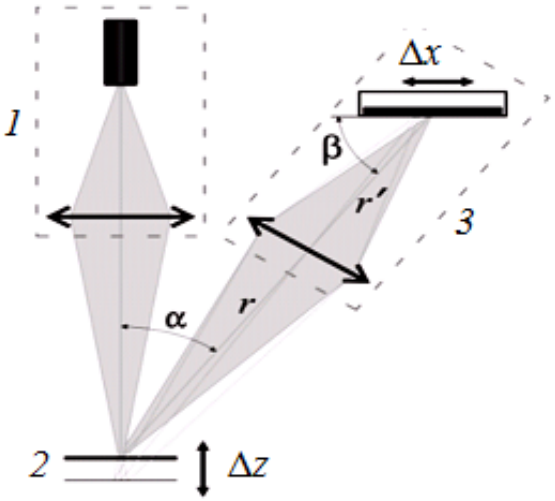

Fig. 1. Schematic diagram of a triangulation meter:
the radiating and receiving channels *1* and *3*, respectively; the controlled surface (*2*); the displacements of the controlled surface (Δz) and a laser spot (Δx); the distances from the controlled surface to the projection lens (r) and from the lens to the photo detector (r')

therefore the measured distance to them have a scale of several micrometers. For example, the accuracy required in the surveying industry is of the order of hundreds of meters.

Industrial dimensional control consists in determining the parameters of metal surfaces, the required control accuracy ranging from a few micrometers (in the nuclear industry) to hundreds of micrometers (in the railway industry).

Each surface also has the property of reflecting or scattering incident radiation. Radiation scattering by the surface of a controlled object is used in triangulation as a physical basis for obtaining information about the distance to this surface. Therefore, the controlled surface is an integral part of the triangulation measuring system.

The third part of the triangulation meter is the receiving channel, consisting of a projection lens and a photodetector. The projection lens generates an image of the probe spot in the plane of the photodetector. The larger the lens diameter *D*, the higher its aperture. In other words, the larger the lens diameter *D*, the more intense the spot image, and the higher its quality. Depending on the specific implementation, either a photodiode array or a position-sensitive receiver is used for capturing the generated image.

The triangulation meter shown in Fig. 2 operates as follows. Emitting channel *1* forms an image of the light spot on controlled surface *2* (*6 – 6`*). Next, the light scattered by the controlled surface enters receiving channel *3*. Thus, an image of the illuminated portion of the controlled surface (light spot) is generated in the plane of the photodetector. If the controlled surface is displaced by Δz (see Fig. 1), the light spot in the plane of the photodetector shifts by Δx. Dependence of the displacement Δz of the controlled surface on the displacement Δx of the light spot in the plane of the photodetector has the following form:

$$\Delta z = r \cdot \sin\varphi / \sin(\alpha - \varphi)$$

where

$$\varphi = \operatorname{arctg}\left(A \cdot \Delta x / (1 + B \cdot \Delta x)\right),$$

$$A = \sin\beta / r', B = -\cos\beta / r',$$

r and r' are the distance from controlled surface *2* to the projecting lens of receiving channel *3*, and that from the lens to the photodetector, despite the fact that the controlled surface is in the center of the range of displacement measurements, respectively.

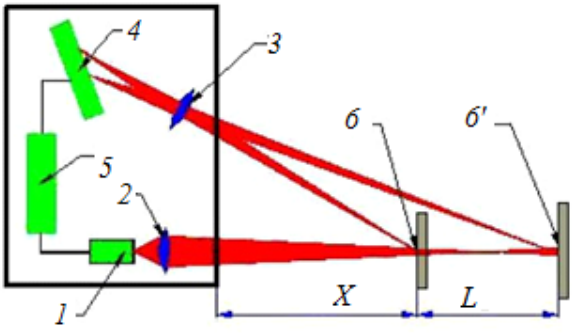

Fig. 2. Principle of operation of the triangulation meter:

the laser (*1*); the lenses of the radiating (*2*) and the receiving (*3*) channels; the dividing plate (*4*); the supply system (*5*); the images of a light spot on the controlled surface (*6 – 6`*)

Software architecture of microcontrollers with ARM core

The ARM core is based on RISC (Reduced Instruction Set Computing) architecture, a processor architecture built on the basis of a reduced set of instructions), using simple and efficient processor instructions that can be executed in a single cycle. The basic concepts of RISC involve shifting the main emphasis in developing applications from hardware to software, since it is much easier to increase application performance by software methods rather than using complex hardware solutions. As a result, programming of RISC processors imposes more stringent requirements for compiler performance compared to CISC architecture (Complete Instruction Set Computing, processor architecture with a wide range of different machine instructions of variable length and different execution times). Microprocessors with CISC architecture (for example, Intel x86) are not so demanding on development software: here the main emphasis is on hardware performance. Fig. 3 shows these differences.

Considering RISC architecture in more detail, we can see that it is based on the following basic principles.

The system of instructions (commands) of the processor. A standard RISC processor has a limited set of instruction types, with each of these instructions executing in a single processor cycle. Individual software algorithms, for example, division, are compiled entirely via software development tools (compilers) or by actual developers. Each processor instruction

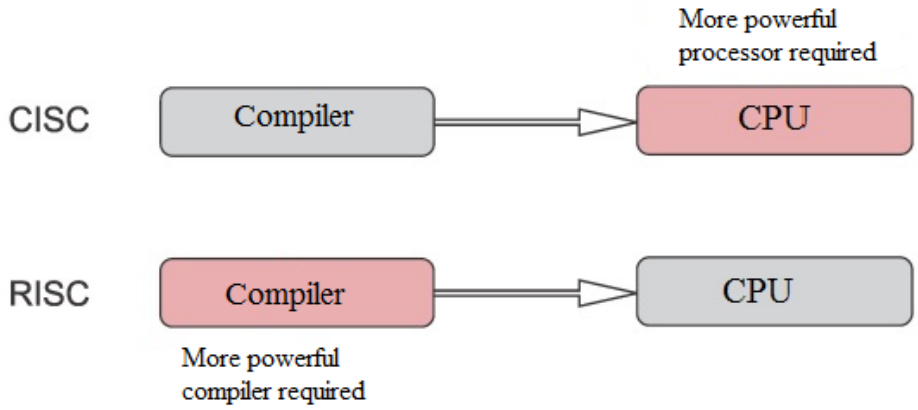

Fig. 3. Architecture of RISC and CISC processes

has a fixed length, which allows to successfully use the pipeline principle to select the next instruction while the previous one is decoded. In contrast, CISC processors have different lengths and can be executed in several machine cycles. Comparing two code snippets for CISC and RISC processors, we can see that the RISC processor needs more instructions. On the other hand, a large number of registers in ARM processors allows computing operations with several variables to be performed very efficiently, since intermediate results of calculations can be placed in registers. In addition, ARM processors can use multiple access instructions for multiple memory locations, which improves the performance of data read/write operations. Additional opportunities for increasing the performance of ARM microprocessors are achieved by using conditional execution instructions, when the next instruction is executed only if the previous instruction set certain flags in the program status register.

Instruction pipeline. Each processor instruction is processed in several stages, which are performed simultaneously. Ideally, in order to achieve maximum performance, the instruction pipeline should move one step in each machine cycle, and decoding of the instruction can be carried out in one step of the pipeline. This approach is different from that adopted for CISC architectures where special microprograms have to be executed to decode instructions.

Using processor registers. RISC processors have many common registers. Each of the registers may contain data or a data address in memory; therefore, registers are local data storages during all operations in the processor. For comparison: CISC processors have a limited set of registers, each with a separate functional purpose, which is why many CISC instructions use a memory cell as one of the operands. For example, the ADD instruction where one of the operands was a memory cell was used for adding two numbers for CISC Intel × 86 processors. Such an instruction requires a lot of machine cycles, reducing the performance of the application, especially if such instructions are used in cyclic calculations. Despite significant differences in architectures, the RISC and CISC architectures are gradually becoming similar. For example, CISC microprocessors are implemented according to RISC principles at the microprogram level. That increases the speed of microinstructions.

The microcontroller stm32f407VET6 and the electrical circuit of the receiving channel

Microcontroller stm32f407VET6. General characteristics of the microcontroller used for operations with the ARM7 core are presented below.

ARM 32-bit Cortex-M4 CPU;

Clock frequency 168 MHz, 210 DMIPS / 1.25 DMIPS / MHz (Dhrystone 2.1);

Support for DSP instructions;

New high-performance AHB-matrix tires;

Up to 1 MB of Flash memory;

Up to 192 + 4 kB SRAM-memory;

Supply voltage of 1.8 − 3.6 V (POR, PDR, PVD and BOR);

Internal RC-generators at 16 MHz and 32 kHz (for RTC);

External clock source of 4−26 MHz and of

32.768 kHz for RTC;

SWD/JTAG debugging modules, ETM module;

Three 12-bit ADCs on 24 input channels (speed up to 7.2 megasamples, temperature sensor);

Two 12-bit DAC;

DMA controller for 16 streams with support for packet transmission;

17 timers (16 and 32 categories);

Two watchdog timers (WDG and IWDG);

Communication interfaces: I2C, USART (ISO 7816, LIN, IrDA), SPI, I2S;

CAN (2.0 B Active);

USB 2.0 FS/HS OTG;

10/100 Ethernet MAC (IEEE 1588v2, MII / RMII);

SDIO controller (SD, SDIO, MMC, CE-ATA cards);

Digital camera interface (8/10/12/14-bit modes);

FSMC-controller (Compact Flash, SRAM, PSRAM, NOR, NAND and LCD 8080/6800); hardware random number generator;

Hardware CRC calculation, 96-bit unique ID;

AES 128, 192, 256, Triple DES, HASH (MD5, SHA-1), HMAC encryption module;

Extended temperature range of 40 – 105 °C.

This controller is selected based on the following parameters:

(i) High performance. High performance is necessary for fast operation of the algorithm for calculating the position of an object.

(ii) High frequency of the core and periphery. The operating frequency of the microcontroller is 168 MHz, which makes it possible to interrogate a linear image sensor with a high frequency, and also allows peripheral data transmission modules to operate at high speeds. The core and peripheral frequencies can be flexibly tuned in this family of controllers, which affects the power consumption of the controller.

(iii) Large number of peripherals. We are primarily concerned with the periphery for data transmission in this study. At the same time, the controller has a large set of different data transfer interfaces, which makes the sensor universal.

Ethernet. The unit is made strictly according to the IEEE802.3 standard. It is possible to transfer data at a speed of 10/100 Mbit/s. Clock synchronization is available: the IEEE1588 v2 protocol is implemented in hardware for this purpose. A fiber optic or copper line requires a third-party transceiver. The PHY transceiver connects directly to the MII or RMII port.

USB (Universal Serial Bus). The system has two separate USB blocks. The first one is USB OTG full-speed, which is fully hardware-implemented and compatible with USB 2.0 standards, as well as OTG 1.0. The USB operates at speeds up to 12 Mbit/s. It is supported in Host/Device/OTG mode. Session Request Protocol (SRP) and Host Negotiation Protocol (HNP) are included.

The second block, USB OTG high-speed, operates in Host/Device/OTG mode with a high speed of 480 Mbps; a transceiver unit operating at high speed through a special ULPI interface is required for this purpose.

USART (Universal Synchronous Asynchronous Receiver Transmitter). Four USART units and two UART (Universal Asynchronous Receiver Transmitter) are integrated in the microcontroller. USART1 and USART6 units allow high-speed data exchange at speeds up to 10.5 Mbit/s. Others support a speed of no more than 5.25 Mbit/s. Thanks to USART, standards such as RS323 and RS485 can be used in the sensor.

Linear Image Sensor ELIS-1024. The ELIS-1024 linear image sensor from Dynamax imaging is used as a photosensitive sensor in the system. This sensor is selected due to its high speed, sufficient resolution with simple controls and low cost.

Its main features are low cost; programmable resolutions of 1024, 512, 256, 128 pixels; high sensitivity; low noise level; clock frequency from 1 kHz to 30 MHz; low dark current; fully customizable clock frequency and frame rate; electrical characteristics: supply voltage of 2.80 – 5.50 V; current consumption of 25 mA; supply voltage of the digital part of 5 V; minimum voltage of the upper logic level of 0.6 V; maximum clock frequency of 30 MHz; saturation output voltage of 4.8 V; output dark voltage of 2.1 V.

This sensor has a resolution control function. The resolution of the sensor can be at 1024, 512, 256, 128 pixels. This is convenient when a high measurement speed is needed.

Eight digital signal lines were created from the microcontroller to operate the sensor:

M1 and M2, controlling the resolution of the sensor and the frame rate and controlled by the table;

Pin PCO-PC5 for operating the image sensor ELIS-1024;

RST (Reset) resets the pixel values and

translates the origin of the pixels to the zero pixel;

SHT (Shutter) is a shutter used to control the exposure of the image sensor;

DATA triggers the image sensor to issue pixels;

RM-pin controls the operation mode of the image sensor, it is directly connected to the total equipment.

Pin CLK are clocking the image sensor; all processes, including laser modulation, occur in the sensor by the clock cycles of this pin; analog signal is used to synchronize with the AD9203 ADC and the microcontroller.

Analog-to-digital converter ADC (AD9203). Data transfer interface (RS485) and receive channel circuit. ADC is an important part of the sensor, the accuracy of measurement directly depends on its conversion accuracy [7, 8]; moreover, it must be fast enough to be able to convert all the signals. We have selected the AD9203 of ADC architecture from Analog Devices. This ADC has a sampling rate of 40 megabytes per second and an accuracy of 10 bits. The ADC transmits data through a parallel interface, which provides greater speed and ease of communication with the microcontroller.

The sensor has several data transfer interfaces for communication with other devices. One of them is UART with the RS485 standard of logical levels. RS485 is a half-duplex multipoint serial data interface. Data transfer is carried out via one pair of conductors using differential signals. The voltage difference between the conductors of one polarity means a logical unit; the difference of the other polarity is zero. RS485 is implemented using the MAX485 chip.

A block diagram for the connection (Fig. 4) and a printed circuit board (Fig. 5) were developed to combine all MCs and other elements of the receiving channel, including the ADC (AD9203) and the data transfer interface (RS485).

Figs. 4 and 5 show the functional and electrical connections between the main blocks and nodes of the electrical circuit of the receiving channel of the triangulation displacement sensor. Evidently, all the electrical connections between the units, including the laser control modules and the ELIS-1024 linear image sensor, are subordinated to the stm32f407VET6 microcontroller.

The electrical circuit was developed in P-CAD (software for Computer Aided Design of electronics by Personal CAD Systems Inc) intended for design of multilayer printed circuit boards, computing and electronic devices. P-CAD includes two main modules: P-CAD Schematic (graphic editor of circuit diagrams) and P-CAD PCB (graphic editor of printed circuit boards), as well as a number of auxiliary programs.

Software STM32Cube TX program.

The STM32Cube TX program is used to configure and further operate the MCs (microcontrollers) and initialize the code of different elements in the circuit board circuit of the receiving channel of the triangulation displacement meter. The program allows to select the necessary MC, specify the clock sources of different buses, initialize the pins, including timers, configure the interrupt. All this is done in graphical mode. The STM32Cube TX program does not allow for errors for operations with hardware. The programmer needs to concentrate directly on solving applied problems: measuring displacements.

The stm32f407vet6 microcontroller is used in the sensor, so ARM Cortex M4 is selected in the Core tab, stm32f4 is in the Series one, stm32f407/417 is in the Line one, LQFP100 is in the Package one. The clock system is configured in the Clock-Configuration tab. The clock of the microcontroller is fully configurable in the STM32Cube TX program. The source of clock signals in this study is an external quartz (8 MHz) generator. At the same time, the system clock frequency (SYSLK) is set to 168 MHz, which is the maximum for our microcontroller.

Asynchronous operation mode is selected to connect the USART serial interface (Universal Asynchronous Receiver-Transmitter) in the USART1 tab; data transfer at a speed of 11500 Bit/s and a data library are connected via USB Full Speed; the integrity of bit parity data is automatically controlled and the parity control is different. When the sum of the number of unit bits in a packet is an even number, and when this sum is odd, USB interruptions are cleared automatically.

Operation of the linear image sensor ELIS-1024. The ELIS-1024 linear image sensor operates in frame-by-frame synchronization mode, when new exposure is set for each new frame.

Data is written to an 8-bit data array with a dimension of 1024 mass-elements [9].

One important point should be noted. The microcontroller operates on 3.3 V, respectively, and the logical unit (high level) will be 3.3 V, and the ELIS-1024 image sensor needs 5 V logic

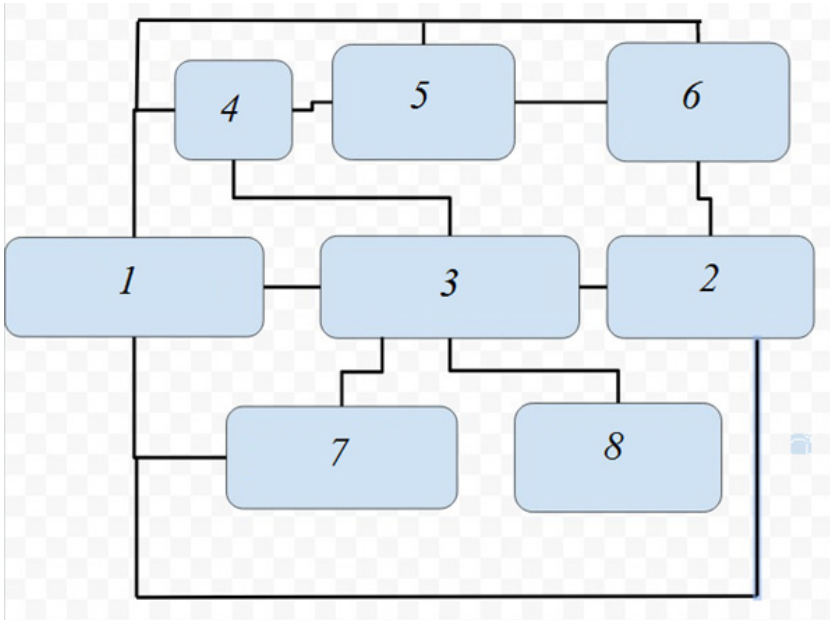

Fig. 4. The electrical block diagram of the receiving channel:
1 is the supply system; *2* is the analog-to-digital converter; *3* is the microcontroller stm32f407vet6; *4* is the interface logic levels RS485 (the main elements of one); *5* is the operational amplifier; *6* is the linear image sensor; *7* is the laser control module; *8* is the data transfer interface

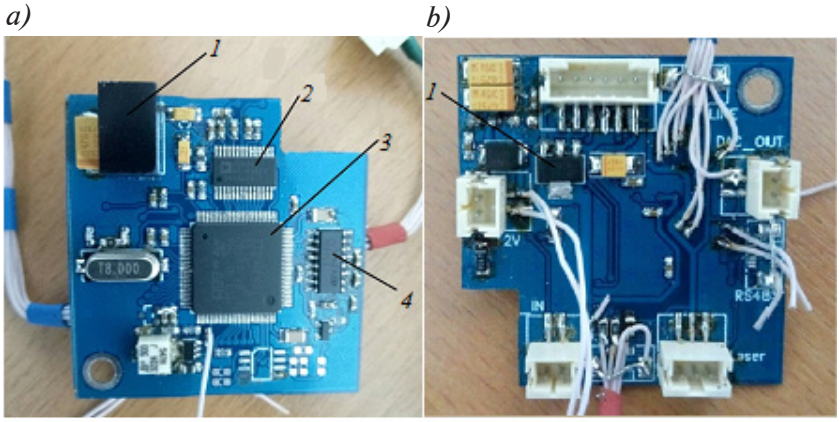

Fig. 5. Appearance of the receiving channel (the face (*a*) and the back (*b*) of the finished printed circuit board with elements);
1 to *4* positions correspond to Fig. 4

levels for normal, fast operation. Therefore, a new level converter should be used. The 74VHCT04AMTCX chip from Fairchild Semiconductor was chosen. In fact, this is not just a converter but also an inverter of levels (6 inverters). This microcircuit was used in the study because it can operate with the required frequencies and voltages. Since the applied microcircuit is an inverter, this is taken into account in the image sensor control function: all signals are inverted. While unity was first supplied earlier for the DATA signal, followed by zero, first zero and then unity is supplied after inversion from the microcontroller.

Processing data from a linear image sensor and calculating distance. After a data array is obtained, it should be processed. According to the triangulation method for finding distance, the beam reflected from the surface of the object passes through the optical system to a linear image sensor. The position of the laser point on the image sensor depends on the distance from the object to the sensor, which is how distance to the object is determined. Therefore, the dis-

tance to the object can be calculated after obtaining data from the image sensor. A graph constructed of data from the linear image sensor clearly shows the laser spot, provided that there is an object in the range visible by the sensor (Fig. 6). The spot has the form of a normal (Gaussian) distribution.

Distribution of the spot can be analyzed to find its exact position on the matrix, which is then translated into the distance to the object. There are several ways to do this.

We used the method for finding the center of mass for a system of material points to calculate the center of the spot in this study. This method allows to calculate the center of the spot with great accuracy that is higher than the resolution of the matrix pixels. The formula for the calculation is as follows:

$$x_C = \frac{\sum m_i \cdot x_i}{\sum m_i}$$

where x_C is the center of the laser spot on the linear image sensor, m_i is the value of the i-th pixel of the spot, x_i is the coordinate of the i-th pixel of the spot.

The center value is calculated only for a region of the spot on the data array with a linear image matrix. The numerator in the function calculating the centroid (the center of the laser spot) is multiplied by 10 because the microcontroller takes longer to perform calculations with fractional numbers.

Application of such a solution allows to perform calculations with larger numbers, it does not matter for the microcontroller how big the number is, allowing to maintain the accuracy of the calculations as a result.

The next steps are to convert the centroid into the metric and convert the position of the laser spot in pixels on the linear matrix into the distance in mm to the sensor. The dependence of the laser spot position (pixels) on the spot – object distance (mm) (it was found from the general optical scheme (see Fig. 7). Calibration tables are introduced to convert distances from subpixels to millimeters.

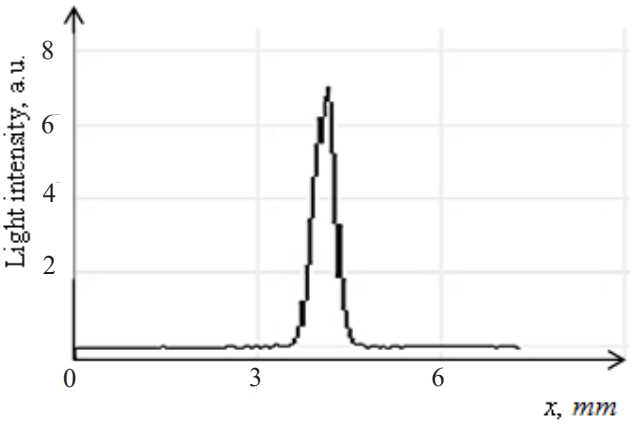

Fig. 6. Laser spot graph (plots of the light intensity versus the x coordinate)

The accuracy of conversion in millimeters depends on the number of elements in the calibration table. The number of table elements in this study was 32.

The bisection method (half division method) was used to search for the range. The half division method allows to exclude half the interval after the each iteration. It is assumed within this method that the function is continuous and has a different sign at the ends of the interval. After the value of the function is calculated in the middle of the interval, one part of the interval is discarded so that the function has a different sign at the ends of the remaining part. Iterations of the bisection method stop if the interval becomes sufficiently small. Since there are 32 values in the calibration table, the method allows to find the interval in just 5 iterations, regardless of the centroid value.

The code of this function consists of about 250 lines, so only part of the code is given. Despite the large code size, the program runs very quickly.

The optical scheme of the displacement sensor

The optical scheme [10] is shown in Fig. 8.

According to Fig. 8, the distance D from the laser (L) to the subject of inquiry (SI) can be found as follows:

$$D = \frac{h}{\tan\theta},$$

where h is the distance between the image sensor (LIS) and the laser (L), θ is the angle between the laser beam and the laser point.

The angle between the laser beam and the returned laser point can be calculated from this formula:

$$\theta = pfc \cdot rpc + ro,$$

where pfc is the number of pixels from the center of the focal plane, rpc is the radian per pixel pitch, ro is the radius offset.

A high reading speed allows to track the position of moving objects, and the resulting accuracy can reach an error of one thousandth of the distance.

An interference filter of 650 nm is installed

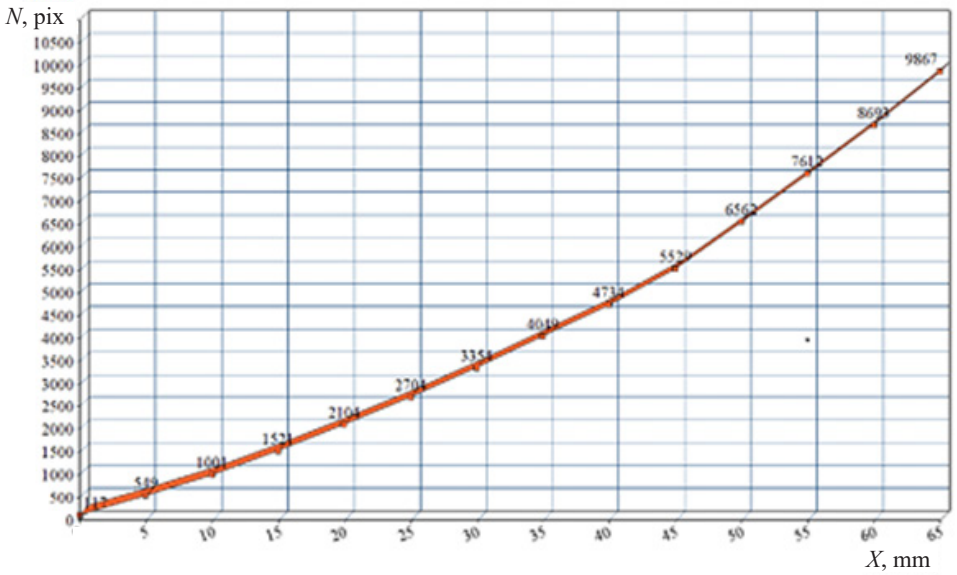

Fig. 7. Plots of the spot position versus the distance from the laser to the measured object (calibration chart)

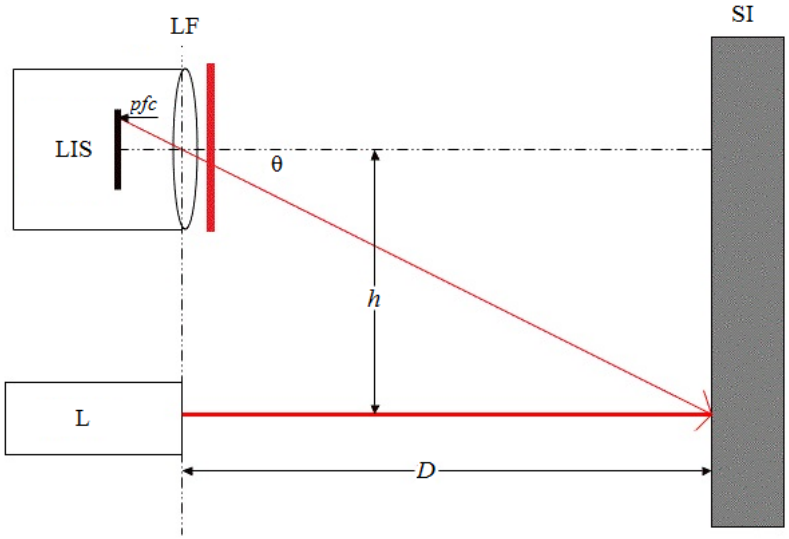

Fig. 8. Optical design of the displacement sensor:
SI – subject of inquiry, L– laser, LF – light filter, LIS – linear image sensor.
Geometric parameters are shown

in front of the lens, which does not transmit light of unnecessary wavelengths, to reduce the influence of external factors and increase accuracy.

Conclusion

The result of the study is a compact triangulation displacement measurement sensor that we have created.

The accuracy of the sensor is 15 – 20 μm, this accuracy is achieved only through correct selection of optics, high-quality filter, accurate calibration on precision equipment, such as CNC machines with digital linear encoders.

The scanning speed is from 3 to 5 thousand measurements per second, which meets most of the needs in the industry. Scanning can be carried out directly on the conveyor without slowing down production.

REFERENCES

1. **Demkin V.N., Stepanov V.A.** Laser methods and means of monitoring the geometric dimensions of products, Measuring Equipment. 69 (2) (2008) 32–35.

2. **Demkin V.N., Stepanov V.A.,** Possibilities of a triangulation laser method for measuring the surface of a complex relief, Metrology. (8) (2007) 32–35.

3. **Demkin V.N., Stepanov V.A.,** Measurement of the roughness profile of materials by the triangulation method, Metrology. (6) (2008) 60–65.

4. **Hausler G.,** Three-dimensional sensors – potentials and limitations, Handbook of computer vision and application, Vol. 1, Academic Press, San Diego, (1999) 485–506.

5. **Crags G., Meuret Y., Danckaert J., Verschaffelt G.,** Characterization of a low-speckle laser line generator, Applied Optics. 51 (20) (2012) 4818–4826.

6. **Tusting R.F., Davis D.L.,** Laser systems and structured illumination for quantitative undersea imaging, Marine Technology Society Journal. 26 (4) (1992) 5–12.

7. **Voisin S., Foufou S., Truchetet F., et al.,** Study of ambient light influence for three-dimensional scanners based on structured light, Optical Engineering. 46 (3) (2007) 030502.

8. **Voegtle T., Schwab I., Landes T.,** Influences of different materials on the measurements of a terrestrial laserscanner (TLS), Int. Archives of the Photogrammetry, Remote Sensing and Spatial Information Science. 37, Part B5 (2008) 1061–1066.

9. **Skvortsov A.V., Mirza N.S.,** Algoritmy postroyeniya i analiza triangulatsiy [Algorithms for constructing and analyzing triangulation], Tomsk State University, Tomsk, 2006.

10. **Demkin V.N., Demkin A.V., Shadrin M.V.,** Device for laser scanning, Patent of Russian Federation, IPC G 01 B 11/24, 2012110279/28; declared 03/16/2012; publ. 11/20/2012. Bull. No. 32, 2012.

Received 16.01.2020, accepted 27.01.2020.

THE AUTHORS

STEPANOV Vladimir A.
Ryazan State University named for S. Ysenin
46 Svobody St., Ryazan, 390000, Russian Federation
vl.stepanov@365.rsu.edu.ru

MOOS Evgueniy N.
Ryazan State University named for S. Ysenin
46 Svobody St., Ryazan, 390000, Russian Federation
e.moos@rsu.edu.ru

SHADRIN Maksim V.
Ryazan State University named for S. Ysenin
46 Svobody St., Ryazan, 390000, Russian Federation
addressworken
m.shadrin@russia.ru

SAVIN Vladislav N.
Ryazan State University named for S. Ysenin
46 Svobody St., Ryazan, 390000, Russian Federation
savin-vladislav@mail.ru

UMNYASHKIN Andrew V.
Ryazan State University named for S. Ysenin
46 Svobody St., Ryazan, 390000, Russian Federation
a.umniashkin@kvantron.com

UMNYASHKIN Nicholas V.
Ryazan State University named for S. Ysenin
46 Svobody St., Ryazan, 390000, Russian Federation
n.umniashkin@kvantron.com

СПИСОК ЛИТЕРАТУРЫ

1. **Demkin V.N., Stepanov V.A.** Laser methods and means of monitoring the geometric dimensions of products // Measuring Equipment. 2008. Vol. 69. No. 2. Pp. 32–35.

2**. Демкин В.Н., Степанов В.А.** Возможности триангуляционного лазерного метода измерения поверхности сложного рельефа // Метрология. 2007. № 8. С. 32–36.

3. **Демкин В.Н., Степанов В.А.** Измерение профиля шероховатости поверхности триангуляционным способом // Метрология. 2008. № 6. С. 60–65.

4. **Hausler G.** Three-dimensional sensors – potentials and limitations. Handbook of computer vision and application. Vol. 1. San Diego: Academic Press, 1999. Pp. 485–506.

5. **Crags G., Meuret Y., Danckaert J., Verschaffelt G.** Characterization of a low-speckle laser line generator // Applied Optics. 2012. Vol. 51. No. 20. Pp. 4818–4826.

6. **Tusting R.F., Davis D.L.** Laser systems and structured illumination for quantitative undersea imaging // Marine Technology Society Journal. 1992. Vol. 26. No. 4. Pp. 5–12.

7. **Voisin S., Foufou S., Truchetet F., Page D., Abidi M.** Study of ambient light influence for three-dimensional scanners based on structured light // Optical Engineering. 2007. Vol. 46. No. 3. P. 030502.

8. **Voegtle T., Schwab I., Landes T.** Influences of different materials on the measurements of a terrestrial laser scanner (TLS) // Int. Archives of the Photogrammetry. Remote Sensing and Spatial Information Science. 2008. Vol. 37. Part B5. Pp. 1061–1066.

9. **Скворцов А.В., Мирза Н.С.** Алгоритмы построения и анализа триангуляции. Томск: Изд-во Томского университета, 2006. 160 с.

10. **Демкин В.Н., Демкин А.В., Шадрин М.В.** Устройство для лазерного сканирования. Патент Российской Федерации. МПК G 01 B 11/24. 2012110279/28; заявлено 03/16/2012; опубликовано 11/20/2012. Бюлл. № 32. 2012.

Статья поступила в редакцию 16.01.2020, принята к публикации 27.01.2020.

СВЕДЕНИЯ ОБ АВТОРАХ

СТЕПАНОВ Владимир Анатольевич – *доктор физико-математических наук, профессор кафедры общей и теоретической физики и методики преподавания физики Рязанского государственного университета имени С.А. Есенина, г. Рязань, Российская Федерация.*
390000*, Российская Федерация,* г. Рязань, ул. Свободы, 46
vl.stepanov@365.rsu.edu.ru

МООС Евгений Николаевич – *доктор технических наук профессор кафедры общей и теоретической физики и методики преподавания физики Рязанского государственного университета имени С.А. Есенина, г. Рязань, Российская Федерация.*
390000*, Российская Федерация, г.* Рязань, ул. Свободы, 46
e.moos@365.rsu.edu.ru

ШАДРИН Максим Владимирович – *аспирант кафедры общей и теоретической физики и методики преподавания физики Рязанского государственного университета имени С.А. Есенина, г. Рязань, Российская Федерация.*
390000*, Российская Федерация,* г. Рязань, ул. Свободы, 46
m.shadrin@russia.ru

САВИН Владислав Николаевич – *инженер кафедры общей и теоретической физики и методики преподавания физики Рязанского государственного университета имени С.А. Есенина, г. Рязань, Российская Федерация.*
390000*, Российская Федерация,* г. Рязань, ул. Свободы, 46
savin-vladislav@mail.ru

УМНЯШКИН Андрей Владимирович – *аспирант кафедры общей и теоретической физики и методики преподавания физики Рязанского государственного университета имени С.А. Есенина, г. Рязань, Российская Федерация.*
390000*, Российская Федерация,* г. Рязань, ул. Свободы, 46
a.umniashkin@kvantron.com

УМНЯШКИН Николай Владимирович – *аспирант кафедры общей и теоретической физики и методики преподавания физики Рязанского государственного университета имени С.А. Есенина, г. Рязань, Российская Федерация.*
390000*, Российская Федерация,* г. Рязань, ул. Свободы, 46
n.umniashkin@kvantron.com